SYNTHESIS, CHARACTERIZATIONS AND RELEASE STUDY OF IBUPROFEN-ENCAPSULATED MAGNETIC NANOCELLULOSE ALGINATE HYDROGEL BEADS

JAGADEESEN SUPRAMANIAM

UNIVERSITI SAINS MALAYSIA

2017

SYNTHESIS, CHARACTERIZATIONS AND RELEASE STUDY OF IBUPROFEN-ENCAPSULATED MAGNETIC NANOCELLULOSE ALGINATE HYDROGELS BEADS

by

JAGADEESEN SUPRAMANIAM

Thesis submitted in fulfillment of the requirements
for the degree of
Master of Sciences

March 2017

ACKNOWLEDGEMENT

Firstly, I would like express my sincere gratitude to my main supervisor, Professor Rohana Adnan and co-supervisor Dr. Noor Haida Mohd Kaus for their continuous support, patience, motivation and guidance during the period of my research work, throughout the completion of my thesis and also for their hard questions which incented me to widen my research from various perspectives.

I would like to thank my family: my parents and to my brothers and sister for supporting me spiritually throughout the writing of this thesis and my life in general. Without their support, it is difficult for me to complete my studies. My sincere thanks also goes to all my friends especially Leong Kwok Yii, Irfan Shah, Voon Sui Yien, Najam Khan, Chong Mui Phin, Miyeko Lotus, Erma, Syikin, Fitrah, Azia, Risha, Sree and Nadirah for their encouragement and advices. I would also like to express my appreciation to the staff of School of Chemical Sciences for their assistance.

Last but not the least, I would like to acknowledge the financial support from the grant number 1001/PIMIA/815099.

TABLE OF CONTENTS

ACKNOWLEDGEMENT ii

TABLE OF CONTENTS iii

LIST OF TABLES vi

LIST OF FIGURES vii

LIST OF ABBREVIATIONS x

LIST OF SYMBOLS xii

ABSTRAK xiv

ABSTRACT xv

CHAPTER 1 - INTRODUCTION 1

1.1 Introduction 1

1.1.1 Rice Husk : Constituents, Disposal and Alternative uses of Rice Husk 5

1.1.2 Nanocellulose 8

1.1.2(a) Alkali Treatment and Bleaching 10

1.1.2(b) Acid Hydrolysis 13

1.2 Cellulose Nanocrystals : Properties and it's Nanocomposite 16

1.3 Hydrogels 18

1.3.1 Classification of Hydrogels 19

1.3.2 Alginate : General Properties 21

1.3.3 Formation of Hydrogels 22

1.4 Drug Delivery System 25

1.4.1 Cellulose Nanocrystals in Drug Delivery System 27

1.5 Kinetic Models Involved in Drug Delivery System 30

1.6 Problem Statements 32

1.7 Objectives 33

CHAPTER 2 - MATERIAL AND METHODS 34

2.1 Raw Materials and Chemicals 34

2.2 Isolation of Cellulose Nanocrystals from Rice Husk 34

2.2.1 Alkali Treatment 35

2.2.2 Bleaching 36

2.2.3 Acid Hydrolysis 36

2.3 Preparation of Magnetic Cellulose Nanocrystal Composite 37

2.4 Preparation of Magnetic Cellulose Nanocrystal - Alginate Beads 37

2.5 Characterizations 39

2.5.1 Fourier Transform Infra-red (FTIR) Spectroscopy 39

2.5.2 X-ray Diffraction (XRD) 40

2.5.3 Transmission Electron Microscopy (TEM) 41

2.5.4 Scanning Electron Microscopy (SEM) 41

2.5.5 Vibrating Sample Magnetometer (VSM) Studies 41

2.6 Beads Diameter Analysis 42

2.7 Textural Profile Analysis 42

2.8 Drug Loading and Encapsulation Efficiencies 42

2.9 Swelling Behaviour 43

2.10 In Vitro Drug Release 44

CHAPTER 3 - RESULTS AND DISCUSSION 45

3.1 Characterizations 45

3.1.1 FTIR Spectroscopic Analysis 45

3.1.2 XRD Analysis 48

3.1.3 TEM Analysis 53

3.1.4 SEM Analysis 55

3.1.5 VSM Analysis 60

3.2 Beads Appearance, Shape and Diameter 63

3.3 Textural Profile Analysis (TPA) 67

3.4 Swelling Behaviour of the Formulated Beads 69

3.5 Drug Loading and Encapsulation Efficiencies 74

3.6 In Vitro Drug Release 76

3.7 Mechanism of Drug Release 78

CHAPTER 4 - CONCLUSION 93

4.1 Conclusion 93

4.2 Future Recommendations 95

REFERENCES 96

APPENDICES 113

LIST OF TABLES

		Page
Table 1.1	Major constituents of rice husk in Malaysia (Rahman et al., 1997.	6
Table 1.2	Summary of some alkali treatment used in the preparation of cellulose with different biomass with different conditions.	11
Table 1.3	Types of acids and reaction condition used in acid hydrolysis of cellulose fibers.	14
Table 2.1	Initial amounts of IBU and m-CNC used in the preparation of the alginate based beads.	38
Table 3.1	The summary of the FTIR absorption bands and their respective assignments.	47
Table 3.2	Percentage of crystallinity from different sources and methods used in calculating the percentage crystallinity.	51
Table 3.3	Magnetization characteristics of m-CNC incorporated alginate hydrogel beads.	62
Table 3.4	Bead diameter analysis formed at a collecting distance of 2 cm, 125 rpm stirring speed and with a flow rate of 1 ml/min.	66
Table 3.5	Mechanical textural parameters of the alginate hydrogel beads (A0) and m-CNC incorporated alginate hydrogel beads (A1-A3).	68
Table 3.6	Drug Loading and Encapsulation Efficiencies of ibuprofen loaded alginate beads formulations.	75
Table 3.7	Estimated parameters obtained by using different mathematical models from prepared formulation in pH 7.4 PBS.	79
Table 3.8	Drug release mechanism from polymeric delivery system of different shape for Korsmeyer-Peppas model (Peppas & Sahlin, 1989).	79

LIST OF FIGURES

		Page
Figure 1.1	Chemical structure of cellulose.	2
Figure 1.2	Aggregated cellulose chains in an ordered region (crystalline region) and disordered region (amorphous region) (Adapted from Oke, 2010).	3
Figure 1.3	Schematic of tree hierarchical structure. ML = middle lamellae between tracheids, P = primary cell wall, S1, S2, S3 = cell wall layers. (Adapted from Moon et al., 2011).	4
Figure 1.4	Schematic representation on the effect of alkali and bleaching treatment on lignocellulosic biomass (Adapted from Tadesse & Luque, 2011)	10
Figure 1.5	The cleaving of amorphous region by acid hydrolysis (Adapted from Oke, 2010).	15
Figure 1.6	Chemical structure of alginate with alternating M and G blocks.	21
Figure 1.7	Egg-box model which formed from ionic crosslinking of alginate and calcium ions (Adapted from Lee & Yuk, 2007).	24
Figure 2.1	A general scheme of isolating cellulose nanocrystals from rice husk	35
Figure 2.2	Experimental setup for the preparation of m-CNC-alginate beads	38
Figure 2.3	United States Pharmacopeia (USP) dissolution apparatus 1 with basket	44
Figure 3.1	FT-IR spectra of magnetic-cellulose nanocrystals (m-CNC), cellulose nanocrystals (CNC), magnetic alginate beads (A10), calcium alginate beads (A0) and pure sodium alginate powder.	46
Figure 3.2.	XRD patterns of m-cellulose nanocrystals (m-CNC) and cellulose nanocrystals (CNC).	49
Figure 3.3	Picture of a magnet acting on magnetic cellulose nanocrytals (m-CNC) and cellulose nanocrystals (CNC).	53

Figure 3.4	TEM images of (a) Cellulose nanocrystals (CNC) and (b) magnetic cellulose nanocrystal (m-CNC).	54
Figure 3.5	SEM images of CNC (a) magnification of 1 kx, (b) magnification of 5 kx and m-CNC (c) magnification of 1 kx, (d) magnification of 5 kx.	56
Figure 3.6	SEM images of A0, A1, A3, A6, and A10 which show the surface morphology of the beads at magnification of 25x (a-e) and beads cross section at magnification of 25x (f-j) and 200x (k-o), respectively.	57
Figure 3.7	M-H curves for m-CNC incorporated alginate hydrogel beads (A1-A10).	61
Figure 3.8	Photographs of (a) freeze dried beads with different formulation and (b) m-CNC. Light microscope images of (c) freeze dried beads, (d) wet beads and (e) photograph of a magnet acting on the beads.	63
Figure 3.9	Shapes of wet beads (a) elongated beads, (b) beads with a tail and (c) spherical beads.	65
Figure 3.10	Swelling profiles of freeze dried beads in PBS, H_2O, and SGF : (a) A0, (b) A1, (c) A3, (d) A6, and (d) A10.	70
Figure 3.11	Time profile of ibuprofen release from of alginate hydrogel beads (A0) and m-CNC incorporated alginate hydrogel beads (A1-A10) in PBS medium (pH 7.4).	77
Figure 3.12	Release kinetic model plots for Higuchi model using the data obtained from in-vitro studies for all the beads formulation for beads A0-A10 (a-e).	80
Figure 3.13	Release kinetic model plots for Korsmeyer-Peppas model using the data obtained from in-vitro studies for all the beads formulation for beads A0-A10 (a-e).	83
Figure 3.14	Release kinetic model plots for and Peppas-Sahlin model using the data obtained from in-vitro studies for all the beads formulation for beads A0-A10 (a-e).	86
Figure 3.15	Variation of the Fickian diffusional exponent, m, with the aspect ratio, 2a/l, where 2a is the diameter and l is the thickness (height) of the device (Adapted from Peppas & Sahlin, 1989)	89

Figure 3.16 Peppas-Sahlin kinetic model plot for alginate hydrogel beads (A0) and m-CNC incorporated alginate hydrogel beads (A1-A10), which was plotted by using Equation 3.9 and data obtained from in-vitro study. 91

LIST OF ABBREAVIATIONS

5-fu	5-fluorouracil
BNC	Bacterial nanocellulose
CNC	Cellulose nanocrystals
DOX	Doxorubicin hydrochloride
DP	Degree of polymerization
EDTA	Ethylenediaminetetraacetic acid
FTIR	Fourier Transform Infrared Spectroscopy
G-block	α-L-guluronic acid
IBU	Ibuprofen
M-block	β-d-mannuronic acid
m-CNC	Magnetic cellulose nanocrystals
MFC	Microfibrillated cellulose
MRI	Magnetic resonance imaging
NOCC	N,O-carboxymethyl chitosan
NSAIDs	Nonsteroidal anti-inflammatory drugs
P(NIPAM-co-AA)	poly(N-isopropylacrylamide-co-acrylic acid)
PBS	Phosphate buffer saline
PLA	Poly(lacticacid)
PNIPAM	Poly(N-isopropylacrylamide)
PVA	Poly(vinyl alcohol)
RGD	Arginine-glysice-aspartic acid
RH	Rice husk

RHA	Rice husk ash
SA	Sodium alginate
SEM	Scanning Electron Microscopy
SF	Sphericity factor
SGF	Simulated gastric fluid
TEM	Transmission Electron Microscope
TET	Tetracycline hydrochloride
TPA	Textural profile analysis
USP	United States Pharmacopeia
VSM	Vibrating Sample Magnetometer
XRD	X-ray Diffraction

LIST OF SYMBOLS

A_a	Area of amorphous peak
A_c	Area of crystalline peak
D	Crystallite size
D_{max}	Longest diameter
D_{min}	Diameter perpendicular to D_{max}
F	Diffusion
H_c	Coercivity values
I_a	Baseline intensity between amorphous and crystalline region
I_c	Intensity of crystalline peak
k	Constant incorporating its geometric character of the matrix
k_1	First order rate constant
k_d	Relaxation rate constants
k_H	Higuchi constant
k_p	Korsmeyer-Peppas constant
k_r	Diffusion rate constant
M_r	Magnetic remanence
M_s	Magnetization values
$Mt/M\infty$	Fraction of drug released at time, t
n	Diffusional exponent
Q	Percentage of the drug release from t = 0 to t > 0
R	Relaxation
R^2	Correlation coefficient
rpm	Revolutions per minute
S	Swelling percentage

W_o	Initial weight of the beads
W_t	Weight of swollen beads at predetermined time
β	Full width of the peak at half the maximum intensity
θ	Diffraction angle
λ	Wavelength
λ_{max}	Maximum absorption wavelength

SINTESIS, PENCIRIAN DAN KAJIAN PELEPASAN IBUPROFEN TERKAPSUL MANIK HIDROGEL NANOSELULOSA ALGINAT MAGNETIK

ABSTRAK

Nanokristal selulosa magnetik (m-CNC) telah disintesis daripada nanokristal selulosa (CNC) yang telah diasingkan daripada sekam padi. m-CNC tersebut telah digabungkan kedalam manik hidrogel alginat untuk aplikasi pelepasan dadah ibuprofen. Pelbagai teknik pencirian seperti FTIR, XRD, TEM, SEM dan VSM telah dijalankan. Puncak baru dapat diperhatikan pada 583 cm^{-1} dalam spektrum FTIR m-CNC menunjukkan kehadiran magnetit dalam bentuk Fe_3O_4 yang juga disokong melalui analisis pembelauan sinar-X. Analisis VSM mendedahkan sifat kemagnetan manik hidrogel alginat (0.027-0.294 emu/g). Analisis profil tekstur (TPA) mendedahkan bahawa penggabungan m-CNC ke dalam manik hidrogel alginat, tidak menjadikan manik rapuh. Peratusan pengembangan yang tinggi sehingga 2477% (PBS, pH 7.4) dan peratusan pengembangan lebih kecil iaitu antara 340-515% (H_2O, pH neutral) dan 402-665% (SGF, pH 1.2) telah diperhatikan. Manik A3 menunjukkan kemuatan dadah dan kecekapan pengkapsulan yang optimum iaitu masing masing 3.2±0.2% dan 38.3±0.1%. Daripada kajian pelepasan ibuprofen, didapati semua manik menunjukkan profil pelepasan pesat dalam 30 min pertama dengan 45-60 % ibuprofen dilepaskan dan pelepasan ibuprofen yang terkawal diperhatikan selepas 30 min dan 100% pelepasan ibuprofen dicapai selepas 6 jam. Mekanisme pelepasan ibuprofen dari manik hidrogel alginat diramalkan dengan menggunakan model matematik seperti Higuchi, Korsmeyer-Peppas dan Peppas-Sahlin. Model Peppas-Sahlin adalah paling sesuai untuk menerangkan mekanisme pelepasan ibuprofen dari manik hidrogel alginat yang terlibat iaitu pembauran dan pengembangan.

SYNTHESIS, CHARACTERIZATIONS AND RELEASE STUDY OF IBUPROFEN-ENCAPSULATED MAGNETIC NANOCELLULOSE ALGINATE HYDROGEL BEADS

ABSTRACT

Magnetic cellulose nanocrystals (m-CNC) were synthesized from cellulose nanocrystals (CNC) that were isolated from rice husk. m-CNC were incorporated into alginate hydrogel beads for ibuprofen release application. Various characterization techniques such as FTIR, XRD, TEM, SEM and VSM were carried out. A new peak observed at 583 cm^{-1} in the FTIR spectrum of m-CNC indicates the presence of magnetite, Fe_3O_4 and corroborated the XRD analysis. VSM analysis reveals the magnetic character of the alginate hydrogel beads (0.027-0.294 emu/g). Textural profile analysis (TPA) results revealed that incorporation of m-CNC into the alginate hydrogel beads, does not make the beads brittle. A high percentage of swelling as much as 2477% (PBS, pH 7.4) and a lower percentage of swelling ranged from 340-515% (SGF, pH 1.2) and 402-665% (H_2O, neutral pH) were observed. Beads A3 showed an optimum drug loading and encapsulation efficiencies which is 3.2 ± 0.2% and 38.3 ± 0.1%, respectively. From the ibuprofen release study, it was found that all the beads showed a burst release profile in the first 30 min and 45-65% of ibuprofen were released and a controlled released profile were observed after 30 min where the 100% of ibuprofen release was achieved after 6 hours. The mechanism of the ibuprofen release from the beads are predicted using mathematical models such as Higuchi, Korsmeyer-Peppas dan Peppas-Sahlin. Peppas-Sahlin model is found to be the best to describe the mechanism of ibuprofen release from the alginate hydrogel beads which are diffusion and swelling.

CHAPTER 1

INTRODUCTION

1.1 Cellulose

Cellulose is the most abundant and renewable biopolymers on the planet earth. Cellulose can be found in many higher plants such as wood fibers (hardwoods and softwoods), grasses (bagasse and bamboo), bast fibers (flax, hemp, jute, banana, kenaf and ramie), leave fibers (agave and sisal), straw fibers (rice, corn and wheat) and seed fibers (cotton and coir) (Biagiotti et al., 2004). It can also be produced by marine animals (e.g. tunicates), algae and bacteria (Iwamoto et al., 2007; Henriksson & Berglund, 2013). Cellulose is the main component found in plant cell wall. It is a rigid and tough substance that plays an important role in providing support and protection to the plant cells, generally together with lignin and hemicelluloses. These three main polymers are closely associated in making up lignocellulosic biomass.

Cellulose is produced when glucose, a product of photosynthesis process in plants, undergoes condensation polymerization process to form a linear homopolymer of anhydroglucose units with β-1,4 glycosidic linkages (C-O-C) (Qiu & Hu, 2013; Chami Khazraji & Robert, 2013; Filson & Dawson-Andoh, 2009). Figure 1.1 illustrates the chemical structure of cellulose. Generally, the chemical structure of cellulose is divided into three parts i.e. non-reducing end, reducing end and cellobiose. The terminal anhydroglucose unit on the left in Figure 1.1 is addressed as the non-reducing end of the cellulose molecule, with an equatorial OH group at C4 atom whereas the terminal on the right is addressed as the chemically reducing end (i.e hemiacetal group) of the cellulose molecule with a OH group at C1 atom. Cellobiose is the basic repeating unit in a cellulose molecule, enclosed in a brackets (Figure 1.1)

and composed of two anhydroglucose units rotated 180° with respect to their ring planes. The number of glucose units or the degree of polymerization (DP) is up to 20, 000, but shorter cellulose chains can occur and are mainly localized in the primary cell walls (Habibi et al., 2010).

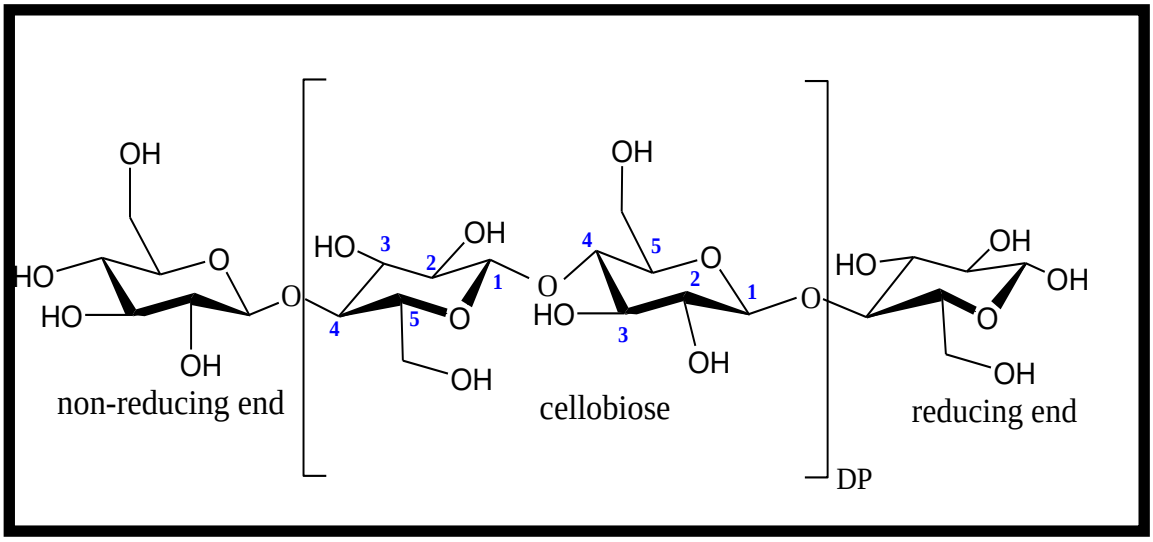

Figure 1.1: Chemical structure of cellulose.

Naturally, cellulose does not exist as an individual molecule, but instead exist as assemblies of individual cellulose chain-forming fibers. This is because, cellulose which is synthesized as individual molecules, will undergo spinning in a hierarchical order at the site of biosynthesis. The cellulose molecule assembles together to form protofibrils. It is then packed into larger units called microfibrils, and assembled into cellulose fibers. However, celluloses from different sources may occur in different packing as dictated by the biosynthesis conditions (Habibi et al., 2010). During the biosynthesis, the cellulose chains aggregated in the microfibrils. Two regions i.e. crystalline and amorphous region are formed during the aggregation of cellulose chains (Figure 1.2). In the ordered region, the cellulose chains are tightly packed together via strong and complex intra- and intermolecular hydrogen-bond network, whereas in disordered region, the cellulose chains are packed loosely and not in order.

Due to the hydrogen bonds, the molecular orientation of cellulose can vary widely and it gives rise to cellulose polymorphs. There are six types of polymorphs that has been identified, namely cellulose I (native cellulose), II, III_I, III_{II}, IV_I, and IV_{II} (Habibi et al., 2010; Moon et al., 2011).

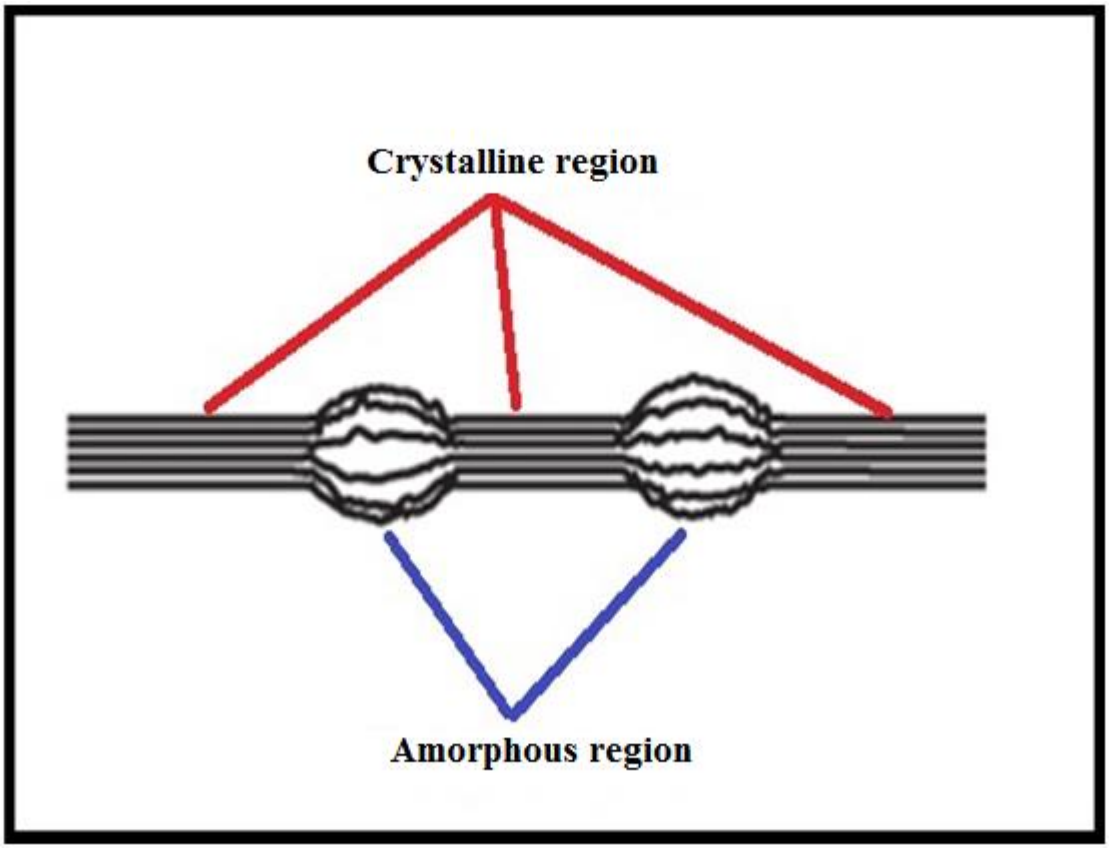

Figure 1.2: Aggregated cellulose chains in an ordered region (crystalline region) and disordered region (amorphous region) (Adapted from Oke, 2010).

The first generation uses of cellulose involved the utilization of cellulose in the form of plants fibers and woods as energy source, building materials, papers and textiles, which took advantage of the hierarchical structure design of trees (Figure 1.3) within these materials (Moon et al., 2011). Natural cellulose based materials have been used as engineering materials for thousands of years. The increase in the number of

industries for forest products, paper, textile etc. indicate the demand of natural cellulose by our society.

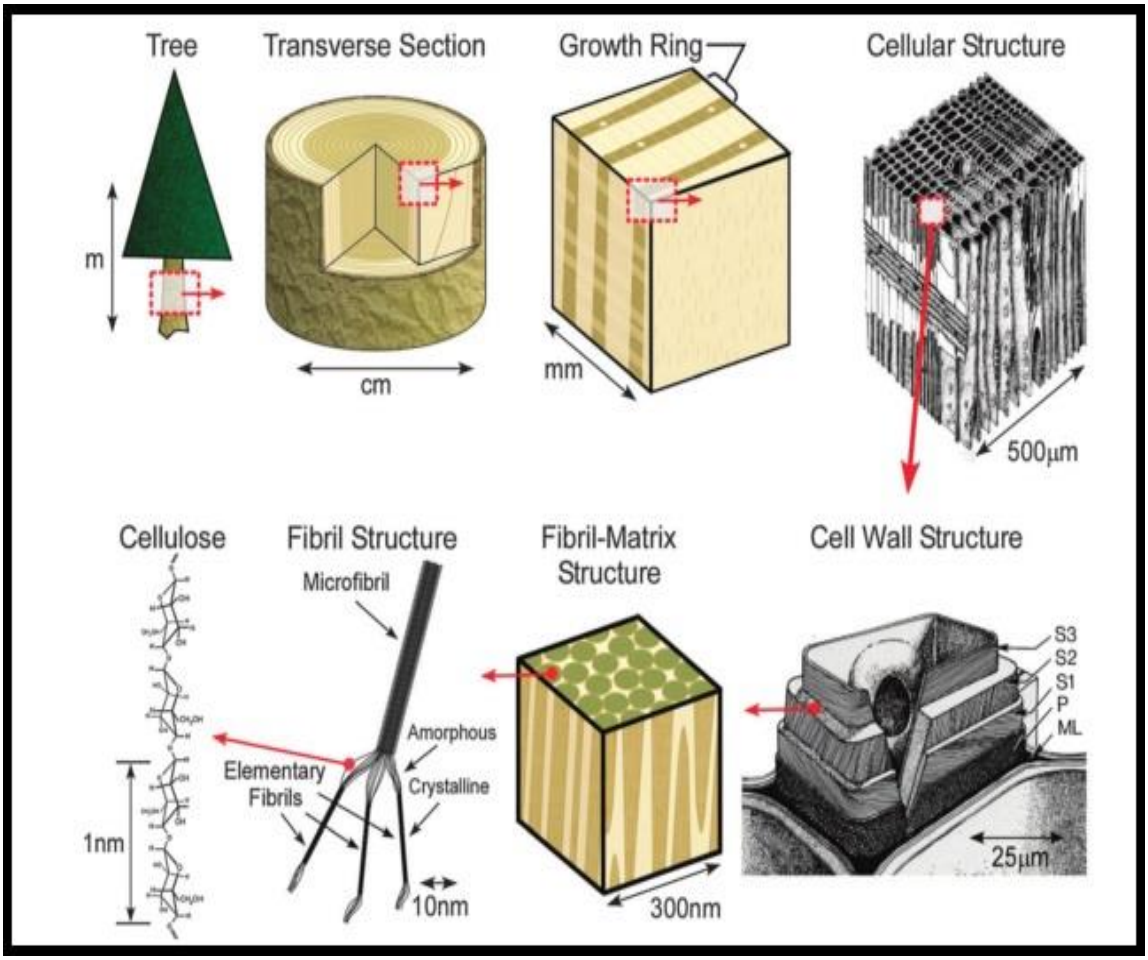

Figure 1.3: Schematic of the tree hierarchical structure. ML = middle lamellae between tracheids, P = primary cell wall, S1, S2, S3 = cell wall layers. (Adapted from Moon et al., 2011).

One of the interesting and important applications of cellulose is as a reinforcement of engineering polymer systems in composite materials (Biagiotti et al., 2004). However, Hubbe and co-workers (2008) reported that celluloses have the tendency to form aggregates during processing. Its incompatiblity with the hydrophobic polymer matrix and water-swellable nature are considered as drawbacks of celluloses. These properties greatly reduce the potential of the natural fibers to be used as reinforcement materials in polymers. In other words, the traditional forest

products have their own uses, but it did not meet the demands of modern society for high performance materials.

Thus, a second generation of cellulose materials requires the removal of the defects associated within the hierarchical structure. On the bright side, there is a basic reinforcement unit that is used to strengthen all subsequent structures within trees, plants, some marine creatures, and algae, which could be extracted and is known as cellulose nanocrystals (CNC) (Moon et al., 2011). CNC is a considered as the new cellulose based building block where cellulose was extracted to a nanoscale and is available for next generation cellulose based composites with new properties and functions, including uniformity and durability (Moon et al., 2011).

1.1.1 Rice Husk : Constituents, Disposals and Alternative uses of Rice Husks.

Rice or paddy is the main source of food in Malaysia. It plays an important role in everyday Malaysian diet by providing energy and supplying nutrient rich complex carbohydrate to human body. Statistically, rice provides 27% of dietary energy supply, 20% of dietary protein and is low in fat (Food and Agricultural Organization of the United Nations, 2002). Besides, the global rice production was approximately 738 million tonnes in 2012. Asia is the biggest rice producer in the world, which contributed 668 million tonnes in year 2012. Although, Malaysia is not a prominent rice-producing country, 2.7 million tonnes of rice were produced (Food and Agricultural Organization of the United Nations, 2012).

Rice husk (RH) are the hard natural sheaths formed on rice grains which served as a protecting layer during their growth. The cultivation of rice produces an agricultural waste RH during rice milling process. During milling process about 78% of weight were produced as rice, broken rice and bran, while the remaining 22% were

received as rice husk (Rice Husk Ash, 2008). More than 75 countries in the world cultivated rice and over 97% of rice husk is generated in developing countries. In 1997, 54 million tonnes of rice husk were generated in China alone (Werther et al., 2000), while, Malaysia produced 3.6 million tonnes of RH annually (Rahman et al., 1997).

RH is not suitable to be reused due to its high abrasion level, non-digestible, low nutritional value, large volume and resistance to degradation (Hashim et al., 1996). The major constituents of rice husks are cellulose, lignin, and ash. These constituents vary depending on the climate and geographic location of growth. Table 1 shows the constituents of RH obtained in Malaysia. Due to its low nutritional value and a significant value of silica content, it is not suitable for animal feed production (Alfaro et al., 2013). Most of the RH produced are simply disposed off as agricultural waste in landfills and is often fermented by microorganisms in wet environment, which results in emission of methane gas (a greenhouse gas) and eventually contributes to global warming (Bhattacharya et al., 1999).

Table 1.1: Major constituents of rice husk in Malaysia (Rahman et al., 1997)

Constituents	Content (%)
Cellulose	32.7
Hemicellulose	20.5
Lignin	21.8
Silica	15.1
Solubles	2.8
Moisture	7.5

Open burning of RH in the fields releases dangerous gases that is harmful to the environment. The toxic compounds such as nitrogen oxides which is responsible for ozone depletion, acid rain, climate change and formation of smog, volatile organic compounds which contribute to the formation of smog, carbon monoxide a greenhouse gas production and particulate matter that contributes to haze are the resultant of open burning (Kadir & Ariffin, 2013). The burning of RH produces rice husk ash (RHA), which are fine particles and can cause breathing problems when inhaled. Open burning of rice husk waste produces toxic chemicals that contribute to several health problems, including asthma, respiratory illnesses, nervous system damage, kidney and liver damage, and reproductive or developmental disorders (Kadir & Ariffin, 2013).

Over the years, many alternative uses of RH and its constituents have been proposed in order to reduce environment and health problems associated with the disposal, either by random disposal or open burning of RH. Some of the alternatives are for the synthesis of activated carbon (Heo & Park, 2015), as bulking agent in compositing (Chowdhury et al., 2014), as fuel to generate power in power reactors (Shafie, 2015), the production of organic compounds such as furfural and levulinic acid (Suxia et al., 2012; Bevilaqua et al., 2013), reducing sugar (Potumarthi et al., 2013), as well as for the production of bioethanol (Lim et al., 2012) and the preparation of silica RH (Yalçin & Sevinç, 2001; Chandrasekhar et al., 2005; Umeda & Kondoh 2010; Pijarn et al., 2010; Mochidzuki et al., 2001; Radhika & Sugunan, 2006)

On the contrary, the exploitation of cellulose content in RH has not been extensively reported so far due to its tedious and multiple preparation steps. Although cellulose accounts for the highest percentage by weight in RH, only few studies on the production of cellulose from RH have been reported (Rezanezhad et al., 2013; Ludueña et al., 2011; Rosa et al., 2012).

1.1.2 Nanocellulose

Nanocellulose can be classified into three main categories i.e. bacterial nanocellulose (BNC), microfibrillated cellulose (MFC) and cellulose nanocrystals (CNC). BNC are three-dimensional web-like/ribbon-like network of nanofibers that are efficiently biosynthesized from aerobic bacteria *Gluconacetobacter xylinius*, also known as *Acetobacter xylinum* (Dayal & Catchmark, 2016; Janpetch et al., 2016; Klemm et al., 2006). BNC can also be secreted extracellularly by certain bacteria belonging to the genera *Agrobacterium*, *Alcaligenes*, *Pseudomonas*, *Rhizobium*, or *Sarcina* (El-Saied et al., 2004). BNC exhibits interesting properties such as good physical properties such as tensile strength (2 GPa) and thermal-expansion coefficient (0.1×10^{-6} K^{-1}) (Ifuku et al., 2009), high crystallinity (Klemm et al., 2011), mechanical strength in the wet state and high water absorption capacity (Janpetch et al., 2016).

MFC are long, flexible and entangled microfibrils (20 nm wide and several micrometers length) that consist of alternating amorphous and crystalline regions. MFC are generally produced from wood pulp by mechanical pressure before and/or after chemical or enzymatic treatment (Klemm et al., 2011). Various terms were used to describe MFC, which include microfibril (Andresen et al., 2006; Andresen & Stenius, 2007; Aulin et al., 2008), microfibril aggregates (Henriksson et al., 2007; Iwamoto et al., 2007), microfibrillar cellulose (Stenstad et al., 2008; Syverud & Stenius, 2009), cellulose nanofiber (Bhatnagar & Sain, 2005; Stenstad et al., 2008), nanofibrillar cellulose (Stenstad et al., 2008; Syverud & Stenius, 2009), cellulose nanofibrils (Ahola et al., 2008) or fibril aggregates (Hult et al., 2001). Several mechanical treatments can be used to convert cellulose fibers to MFC, namely, refining and high pressure homogenizing (Alain et al., 2000; Zuluaga et al., 2007), grinding (Panthapulakkal & Sain, 2012), cryocrushing (Bhatnagar & Sain, 2005),

microfluidization (Ferrer et al., 2012), and high intensity ultrasonication (Qua et al., 2011). Although there are many mechanical treatments that can be used to produce MFC from cellulose fiber, most of the mechanical treatments require high energy to complete the process (Chinga-Carrasco, 2011).

Cellulose Nanocrystals (CNC) are cellulose-based nanoparticles that are highly crystalline in nature. The main difference between MFC and CNC, is amorphous region is present in MFC and absent in CNC. This makes CNC less flexible compared to MFC. CNCs are also reported in different names by different authors such as microcrystalline cellulose (Araki et al., 1998), nanocellulose (Mandal & Chakrabarty, 2011), cellulose nanowhiskers (Oksman et al., 2011) and nanocrystalline cellulose (Chang et al., 2010). Several lignocellulosic biomasses have been used to isolate CNC from cellulose that was extracted from wood (Beck-Candanedo et al., 2005), potato peel waste (Chen et al., 2012), pineapple leaf (Cherian et al., 2010), cotton (Meyabadi et al., 2014), mango seed (Henrique et al., 2013), kenaf bast fibers (Kargarzadeh et al. 2012), garlic skin (Reddy & Rhim, 2014), white coir (Nascimento et al., 2014), coconut husks (Rosa et al., 2010), and mulberry (Li et al., 2009). The isolation of CNC from lignocellulosic biomass involves three main steps i.e alkali treatment, bleaching and acid hydrolysis as discussed in the following section.

1.1.2(a) Alkali treatment and bleaching

Lignocellulosic biomasses are mainly composed of three different types of polymers, namely cellulose, hemicellulose and lignin, which are closely related with each other. Basically, cellulose can be found in microfibrils which is enclosed by hemicellulose and lignin (Rong et al., 2001; Vignon et al., 2004). Cellulose is protected by hemicellulose and lignin, therefore in order to extract cellulose, removal or hemicellulose and lignin is necessary. Thus, the major objective of alkali treatment (mercerization) and bleaching (delignification) are to disrupt the structure of hemicellulose and lignin in the biomasses. Once lignin and hemicellulose have been removed, cellulose can be subjected for other treatments such as acid hydrolysis. Figure 1.4 shows the schematic representation of the alkali and bleaching treatment on the lignocellulosic biomass.

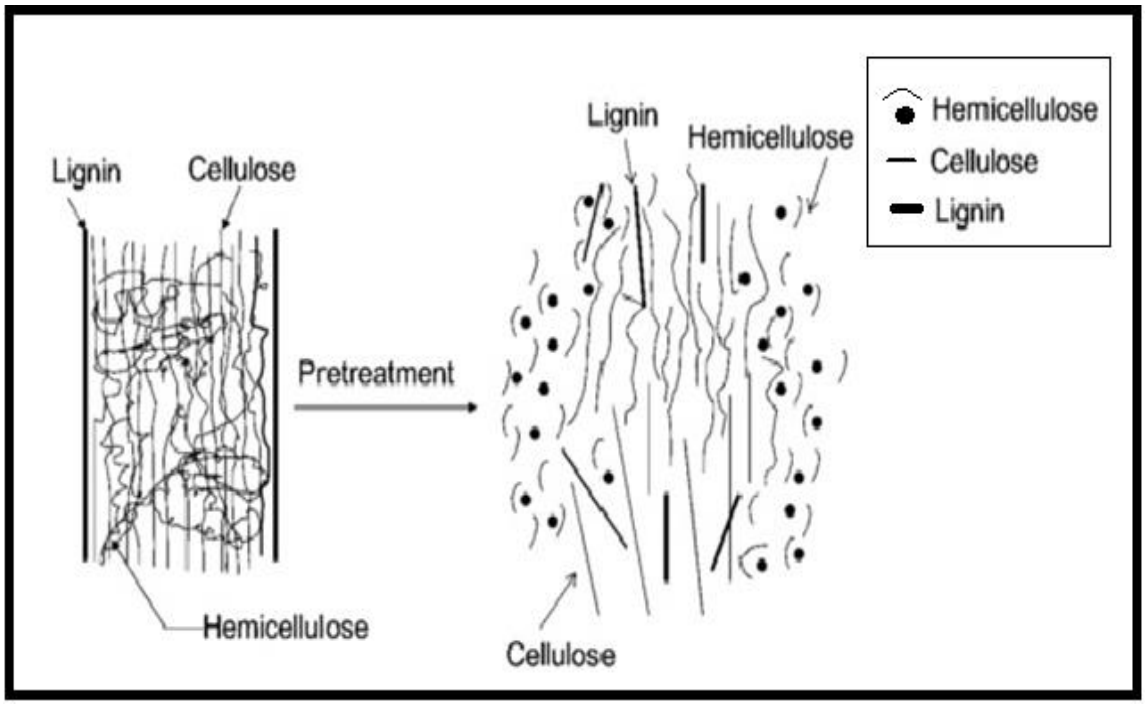

Figure 1.4: Schematic representation on the effect of alkali and bleaching treatment on lignocellulosic biomass (Adapted from Tadesse & Luque, 2011).

Generally, alkali treatment is effective on agricultural residues and herbaceous crops such as rice husks, corncobs and etc (Silverstein et al. 2007). Alkali treatments with different reaction temperature, time, concentration and type of chemicals employed in the lignocellulosic biomass are summarized in Table. 1.2. The most common chemical used in alkali treatment of lignocellulosic biomass is NaOH. Most of the hemicelluloses will be dissolved or solubilized in NaOH during alkali treatment (Silverstein et al., 2007; Dufresne et al., 1997). The solubilization of hemicelluloses is expected to improve the acid hydrolysis process.

Table 1.2: Summary of some alkali treatment used in the preparation of cellulose with different biomass with different conditions.

Biomass	Conditions	References
Sugarcane bagasse	100 °C, 17.5% NaOH, 5 h	Mandal & Chakrabarty, 2011
Poplar	65 °C, 0.5:1 $Ca(OH)_2$, 4 w	Kumar et al., 2009
Corn stover	55 °C, 0.5:1 $Ca(OH)_2$, 4 w	Kumar et al. 2009
Mango seed	100 °C, 2% NaOH, 4 h	Henrique et al., 2013
Sorghum Bagasse	25 °C, 1 % NaOH, 1 h 25 °C, 2 % NaOH, 1 h 25 °C, 5 % NaOH, 1 h	Wu et al., 2011
Rice straw	20 °C, 6 % NaOH, 3 w	He et al., 2008

Bleaching or delignification is a process where the lignin residues are completely removed from the lignocellulosic biomass and to whiten the pulp (Dufresne et al., 1997). There are three different chemicals that can be used for bleaching, namely, oxidizing agents, ionic liquids and organosolv. Three main oxidizing agents that have been used by several researchers, namely, sodium chlorite, $NaClO_2$ (Nasri-Nasrabadi et al., 2014; Zhang et al., 2014; Mandal & Chakrabarty, 2011; Oksman et al., 2011), hydrogen peroxide, H_2O_2 (Correia et al., 2013; Lu &

Hsieh, 2012) and peracetic acid, $C_2H_4O_3$ (Abdel-Halim & Al-Deyab, 2011; Yin et al., 2011). This treatment is mainly and aggressively focused on lignin. The oxidizing agents catalyse the cleaving of the lignin's aromatic ring which then solubilize and dissolve the lignin, thus whitening the biomass (Abdel-Halim & Al-Deyab, 2011; Yin et al., 2011; Lu & Hsieh, 2012).

Organosolv treatment is a process where lignin and hemicellulose will be solubilized, dissolved and degraded in the presence of organic solvents. The organic solvents are used as a dissolving agent to solubilize the lignin and hemicellulose under heating, leaving pure solid residue as the end product. Some of the organic solvents commonly used are methanol, ethanol, acetone, ethylene glycol and ethyl acetate (Zhao et al., 2009). Most of the organic solvent used have low boiling points. However, this treatment is not economically feasible to be employed. Extensive washing is needed to avoid re-precipitation of dissolved lignin, leading to cumbersome washing arrangements. Besides that, organic solvents are usually expensive. Furthermore, the recovery of organic solvent causes high energy consumption (Zheng et al., 2009; Zhao et al., 2009).

In addition to that, ionic liquids are reusable liquid salts at room temperature, and are stable up to approximately 300 $^{\circ}$C. Ionic liquids typically composed of inorganic anion and organic cation, which can be tuned to generate different dissolving capacity for targeted components (Li et al., 2010). Ionic liquids that are involved in cellulose dissolution and biomass pretreatment are 1-alkyl-3-methylimidazolium $[C_nmim]^+$, 1-alkyl-2,3dimethylimidazolium $[C_nmmim]^+$, 1-allyl-3-methylimidazolium $[Amim]^+$, 1-allyl-2,3-dimethylimidazolium $[Ammim]^+$, 1-butyl-3-methylpyridinium $[C_4mPy]^+$, and tetrabutylphosphonium $[Bu_4P]^+$ with n = number of carbons in the alkyl chain (Zavrel et al., 2009; Tadesse & Luque, 2011). Due to the

fact that the extraction of cellulose from non-cellulosic material is complicated, the composition of anion and cation of ionic liquids need to be altered in a way that only hemicellulose and lignin will be solubilized (Lee et al., 2009).

In a nutshell, the alkali treatment and bleaching processes promote the selective solubilization of non-cellulosic components. Lignin is oxidized in the presence of oxidizing agent, while hemicellulose is dissolved and solubilized in alkali. On the other hand, organosolv dissolved both of the non-cellulosic components. Although ionic liquid can dissolve both cellulose and non-cellulosic components, the composition of ionic liquid can be tuned, so that the affinity towards non-cellulosic component can be increased.

1.1.2(b) Acid hydrolysis

CNCs are obtained when the cellulose microfibrils, the product of alkali treatement and bleaching, undergo acid hydrolysis process with strong mineral acids such as hydrochloric acid and sulphuric acid. Factors that govern the efficiency of acid hydrolysis are type of acid and its concentration, hydrolysis time and temperature applied (Table 1.3). Even though, various acids have been used, sulphuric acid and hydrochloric acid are the most common acids reported in literature. The amorphous region of the cellulose microfibrils have less resistance towards acid attack compared to the crystalline region (Habibi et al., 2010). Figure 1.5 illustrates the removal of amorphous region from cellulose upon acid hydrolysis.

Table 1.3: Types of acids and reaction condition used in acid hydrolysis of cellulose fibers.

Type of acids	Reaction conditions	Reference
Sulfuric acid	6.5 M, 60 °C, 2 hr, 1: 10 (fiber : acid)	Zhang et al., 2014
	48 and 64 wt%, 1 hr, 45 °C, 1: 10 (fiber : acid)	Han et al., 2013
	11.21 M, 10 min, 45 °C, 1: 20 (fiber : acid)	Henrique et al. 2013
Hydrochloric acid	6.0 M, 110-120 °C, 2-4 hr, 1: 40-80 (fiber : acid), hydrothermal	Yu et al., 2013
	6.5 M, 60 °C, 2 hrs, 1: 10 (fiber : acid)	Zhang et al., 2014
Phosphoric acid	6.5 M, 60 °C, 2 hrs, 1: 10 (fiber : acid)	Zhang et al., 2014
	6.2-10.7 M, 50 or 100 °C, 30-90 min,	Camarero Espinosa et al., 2013
Hydrobromic acid	1.5-4 M, 100 °C, 1-4 hrs, 1: 5 (fiber : acid)	Sadeghifar et al., 2011
Phosphotungstic acid	50-85 %, 90 °C, 15-30 hr, 1: 20 (fiber : acid)	Liu et al., 2014

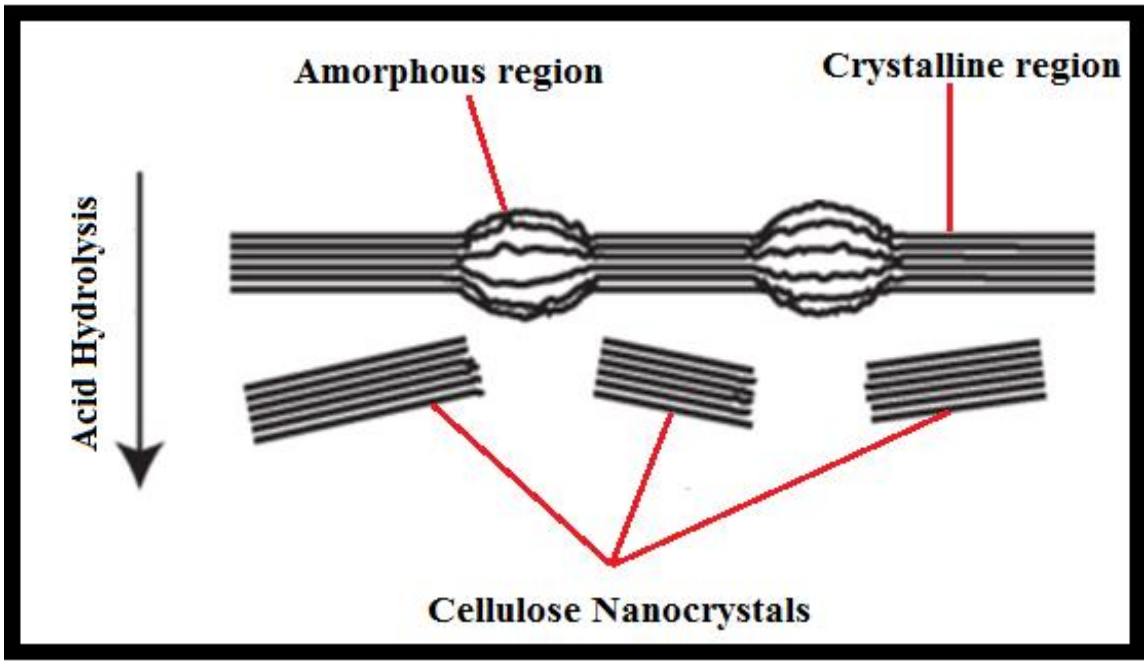

Figure 1.5 : The cleaving of amorphous region by acid hydrolysis (Adapted from Oke, 2010).

During acid hydrolysis, the amorphous region is dissolved, whereby promoting the hydrolytic cleavage of β-1,4 glycosidic linkages by hydronium ion (H_3O^+), thus leaving the individual crystallite of cellulose from the crystalline region (Kargarzadeh et al., 2012; Abraham et al., 2011). One of the advantages of using sulfuric acid as the hydrolyzing agent is the esterification process on the surface of the hydroxyl group involving the grafting of anionic sulfate ester groups. The presence of these negatively charged groups gives electrostatic stability which promotes their dispersion in water and stability of CNC suspension (Beck-Candanedo et al., 2005; Elazzouzi-Hafraoui et al., 2008).

On the other hand, CNC obtained from hydrolysis using hydrochloric acid lacks surface charges due to the formation of hydrogen bonding between the surface of hydroxyl groups, where CNC-CNC interactions form and often flocculate in the

medium (Habibi et al., 2010; Camarero Espinosa et al., 2013). One of the disadvantages of using sulfuric acid as hydrolyzing agent is that the CNC obtained has low thermostability due to the sulphate group. In a nutshell, acid hydrolysis is a well known and widely used process, where the amorphous region is hydrolyzed to isolate CNC. This process only requires a mild reaction conditions and it is not time consuming, Table 1.3. However, with poor handling, it might lead to an over-hydrolysis of cellulose fibers, and the desired product will not be obtained.

1.2. Cellulose Nanocrystals : Properties and it's Nanocomposites

In general, cellulose nanocrystals (CNCs) are rod like nanoparticles that are isolated from cellulose by acid hydrolysis. CNCs are highly crystalline in nature, have high aspect ratio (ratio of length of crystallite, L to the diamater of crystallite, D), low in density, biodegradable and biocompatible (Silvério et al., 2013). CNCs are considered as good reinforcing agent due to its properties such as large specific surface area and high stiffness. The axial Young modulus of CNCs (100–200 GPa) is theoretically stronger than steel and is similar to Kevlar (Lin & Dufresne, 2014; Yu et al., 2012; Habibi et al., 2010; Mandal & Chakrabarty, 2011). Besides, CNC also exhibits self assembly properties where chiral nematic structures were observed when the suspension was viewed under polarized optical microscope. In addition to that, the surface of CNCs are composed of hydroxyl groups which can be easily subjected to chemical modification. Some of the examples of the modifications are esterification (Habibi, 2014), etherification (Habibi et al., 2010), silylation (Siqueira et al., 2010), 2,2,6,6-tetramethylpiperidine-1-oxyl radical (TEMPO)-mediated oxidation and polymer grafting (Araki et al., 2001).

Recently, nanofillers that are derived from natural resources such as CNC, hydroxypropyl methylcellulose (HPMC) and starch are incorporated into biopolymer to form biopolymer nanocomposites in order to improve its mechanical properties (Bilbao-Sainz et al., 2011). Biopolymers are polymers that can undergo biodegradation and they are considered as an alternative for synthetic polymers (Jana et al., 2011). In recent years, researchers have developed several types of CNC based nanocomposites e.g. poly(lacticlacid) (PLA)/surfactant-modified CNC (Fortunati et al., 2014), CNC/nitrile rubber (Cao et al., 2013), CNC/poly(vinyl alcohol) (PVA) hydrogels (Tanpichai & Oksman, 2016), CNC/iron oxide (Sadasivuni et al., 2016), CNC/PVA films (Silvério et al., 2013) and more.

Many applications for CNCs have been reported, but most of the studies focus on their mechanical properties as reinforcing element. Bilbao-Sainz et al., (2011) reported that by using CNC as filling material, the HPMC/CNC nanocomposites film exhibited better mechanical properties. Besides, Chen et al., (2015) reported that the introduction of CNC into nitrile rubber foams enhanced the mechanical properties of the composites. In addition to that, Chen et al., (2012) concluded that even at low CNC loadings of 1–2 wt% into a biopolymer matrices such as starch and PVA, the mechanical properties such as the Young's modulus were enhanced by 19% and 33%, respectively. Based on these findings, it can be concluded that the incorporation of CNC into polymer matrix will enhance the mechanical properties of the nanocomposite and CNC can be considered as one of the promising nanofillers.

1.3. Hydrogels

Hydrogels are 3-D network of polymers that are made of natural or synthetic materials possessing a high degree of water or biological fluids retention or absorption capacity (Peppas et al., 2000). The presence of hydrophilic groups such as –OH, –CONH–, –$CONH_2$–, and –SO_3H in polymers forming hydrogel structures are the primary reasons which explain the water absorption capability of hydrogels (Peppas & Khare, 1993). Generally, the 3-D network of the hydrogels are composed of homo-polymer or co-polymer and are insoluble. The presence of chemical crosslinks (tie-point joints), or physical crosslinks, such as entanglements or crystallite makes the hydrogel insoluble. Besides that, physical crosslinking via hydrophobic interactions, ionic complexation, physical domain junctions and hydrogen bonding provides the network structure and physical integrity of the hydrogels (Peppas et al., 2000), whereas in chemical crosslinking, the polymer chains are covalently bonded via a crosslinking agent such as ethylene glycol and divinyl benzene (Peppas & Khare, 1993).

Hydrogels possesses several interesting characteristics such as their ability to respond to external stimuli as temperature, pH, ionic strength, electric or magnetic fields depends on the nature of polymer chains and the ability to swell under aqueous media. These properties makes them useful in applications such as controlled drug delivery. In drug delivery systems, hydrogel offers many advantages, such as sustained and prolonged action in comparison to conventional drug delivery systems, and decreased side-effects (Ribeiro et al., 2014; Sandeep et al., 2012). In addition to that, the drug encapsulated using hydrogels can be targeted to specific site like colon and mucosa in the colon is protected from irritating drugs such as ibuprofen. Ultimately, hydrogels can also improve drug utilization and patient compliance, reduce daily cost

to patient due to fewer dosage units required by the patient in therapy and drugs adapts to suit circadian rhythms of body functions or diseases (Sandeep et al., 2012).

1.3.1 Classification of Hydrogels

Hydrogels can be classified based on their physical properties, response, ionic charges, preparation methods and type of crosslinking i.e. physical or chemical crosslinking (Qiu & Park, 2012). Chemical crosslinked hydrogels can be obtained by radical polymerization and the chemical reaction between the functional groups (mainly OH, COOH, NH_2) of the natural or synthetic polymers and crosslinking agent such as glutaraldehyde and adipic acid dihydrazide (Sandeep et al., 2012). On the other hand, physical crosslinking are divided into crosslinking by ionic interactions and crosslinking by crystallization. One of the example of crosslinking by ionic interaction is alginate polymer. Poly(vinyl alcohol) (PVA) is a great example of water soluble polymer that can be crosslinked by crystallization. The aqueous solution of PVA exhibits itself as gel with a low mechanical strength at room temperature. However, upon freeze-thawing process a strong and elastic gel is formed. Gel formation is ascribed to the formation of the PVA crystallites that act as physical crosslinking sites in the network (Lozinsky & Plieva, 1998).

The usage of crosslinking agents in chemically crosslinked hydrogels, often affects the integrity of the encapsulated or entrapped substances. Furthermore, these crosslinking agents also are toxic compounds which need to be removed before the hydrogels can be applied. On the contrary, physically crosslinked hydrogel can be produced at room temperature and physiological pH, which is ideal for the encapsulation of living cells (Thu et al., 1996) and for the release of proteins (Albarghouthi et al. 2000). In addition, the usage of metallic ion yield a stronger

hydrogel. Due to the pros and cons of physical and chemical crosslinking, physically crosslinked hydrogels is preferred in drug delivery applications.

Stimuli responsive hydrogels are divided into three i.e., physically responsive, biochemically responsive and chemically responsive hydrogels. These hydrogels respond to the environment stimuli and experience changes in their growth, network structure, mechanical strength and permeability (Peppas et al., 2000; Gil & Hudson, 2004). Temperature sensitive hydrogels are one of the examples of physically responsive hydrogels. This kind of hydrogels has the ability to swell and shrink when the temperature change in the surrounding fluid which means the swelling and deswelling behaviour mostly depend on the surrounding temperature. The most common polymer that is used in temperature responsive hydrogels is N-isopropylacrylamide (NIPAAm) (Laftah et al., 2011; Gil & Hudson, 2004).

Antigen responsive hydrogels are biochemically responsive hydrogels that are designed by grafting antigens on the polymer to deliver biomolecules to a targeted site. Miyata and co-workers (2002) reported that antigen responsive hydrogel is prepared by grafting the antigen, imunoglobulin G (IgG) and the antibody, goat anti-rabbit IgG (GAR IgG) to the polymer. The authors reported that, the presence of free anti rabbit IgG in the buffer solution, induce the swelling of antigen-antibody entrapment hydrogel. Thus, the antigen–antibody entrapment hydrogel showed antigen-sensitive behavior.

pH responsive hydrogels are the main examples of chemically responsive hydrogels. These kind of hydrogels swell and deswell upon pH change in the environment. Dolatabadi and co-workers (2006) reported that the swelling percentage of alginate-N,O-carboxymethyl chitosan (NOCC) gel beads coated with chitosan at

pH 7.4 is higher at pH 1.2. These results indicates that the hydrogel is sensitive to pH and can be considered as pH responsive hydrogels.

1.3.2 Alginate : General properties

Alginate is a well known natural polymer that consist of mannuronic and glucuronic acid residues and can be crosslinked by calcium ions (El-Aassar et al., 2014; Cavallaro et al., 2013; Caballero et al., 2014; Khazaeli et al., 2008). It is a linear, unbranched and natural occuring polysaccharide co-polymer composed of 1,4-linked β-D-mannuronic acid (M-block) and α-L-guluronic acid (G-block), which are found in varying composition and sequence (Figure 1.6) (Caballero et al., 2014).

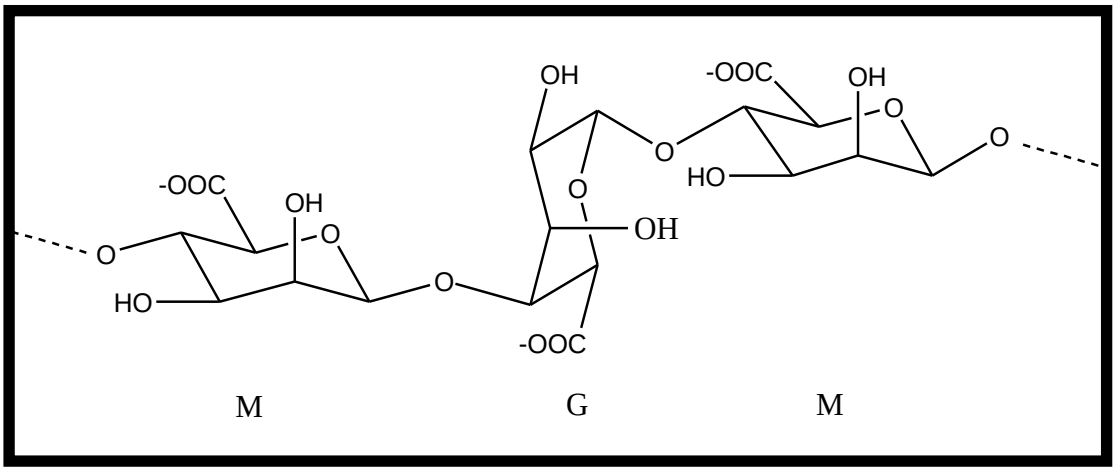

Figure 1.6: Chemical structure of alginate with alternating M and G blocks.

Most of the commercially available alginate are extracted from brown algae (*Phaeophyceae*), including *Laminaria digitata*, *Laminaria hyperborea*, *Laminaria japonica* and *Macrocyctis pyrifera* (Fertah et al., 2014), while bacterial alginate can be produced from *Azotobacter* and *Pseudomonas* via biosynthesis (Gacesa, 1998; Peña et al., 2008). Remminghorst and colleagues (2006) reviewed that alginate biosynthesis started when carbon source is oxidized to acetyl coenzyme A (acetyl-CoA), then

converted to fructose-6-phosphate, and then eventually converted to GDP-mannuronic acid, which acts as a precursor to alginate synthesis (Remminghorst & Rehm, 2006).

One of the interesting properties of alginate is its capability to chelate with divalent ions to form hydrogels beads. Basically there are three types of junctions involved in the formation of hydrogel beads, namely, GG/GG junctions, MG/MG junctions and mixed GG/MG junctions (Donati et al., 2005), refer also Figure 1.6. The formation of hydrogel beads occurs when the G-blocks form a strong and tight junctions with the divalent cations (Sikorski et al. 2007). Besides G-blocks, MG blocks can also form junctions, but the junction is weaker compared to the G-blocks (Donati et al., 2005). Divalent cations such as Ca^{2+}, Sr^{2+} and Ba^{2+} have been used to produce alginate hydrogels beads. However, Mørch and co-workers (2006) reported that the affinity of alginates towards divalent ions decreases in the following order: Pb > Cu > Cd > Ba > Sr > Ca > Co, Ni, Zn > Mn. Ca^{2+} is the most commonly used divalent cations to produce alginate hydrogels beads.

1.3.3 Formation of alginate hydrogels beads

Generally hydrogels are produced by cell crosslinking, covalent crosslinking, thermal gelation, and ionic crosslinking. Cell cross-linking form when alginate is modified with cell adhesion ligands which then bind with multiple polymer chains leading to a hydrogel formation. Lee and co-workers (2003) successfully produced a cellular cross-linked hydrogel by adding cells to an arginine-glysice-aspartic acid (RGD) modified alginate solution which subsequently generates the cross-linked network structure via specific receptor ligand interactions without any cross-linking agents. Their results revealed that interactions between cell receptors and adhesion ligands can be used to form a reversible gel system, in which once the gel structure is